This paper is published as part of a *PCCP* themed issue on characterisation of adsorbed species

Guest Editors: Petr Nachtigall and Carlos Otero Arean

Editorial

Perspective

Communications

Papers

Phys. Chem. Chem. Phys., 2010
DOI: 10.1039/c000988a

Adsorption of light hydrocarbons in the flexible MIL-53(Cr) and rigid MIL-47(V) metal–organic frameworks: a combination of molecular simulations and microcalorimetry/gravimetry measurements
N. Rosenbach Jr, A. Ghoufi, I. Déroche, P. L. Llewellyn, T. Devic, S. Bourrelly, C. Serre, G. Férey and G. Maurin, *Phys. Chem. Chem. Phys.*, 2010
DOI: 10.1039/c001173h

Role of dispersive interactions in the CO adsorption on MgO(001): periodic B3LYP calculations augmented with an empirical dispersion term
Bartolomeo Civalleri, Lorenzo Maschio, Piero Ugliengo and Claudio M. Zicovich-Wilson, *Phys. Chem. Chem. Phys.*, 2010
DOI: 10.1039/c001192d

Nature and role of surface carbonates and bicarbonates in CO oxidation over RuO_2
Hangyao Wang and William F. Schneider, *Phys. Chem. Chem. Phys.*, 2010
DOI: 10.1039/c001683g

Experimental and theoretical determination of adsorption heats of CO_2 over alkali metal exchanged ferrierites with different Si/Al ratio
Arnošt Zukal, Angeles Pulido, Barbara Gil, Petr Nachtigall, Ota Bludský, Miroslav Rubeš and Jiří Čejka, *Phys. Chem. Chem. Phys.*, 2010
DOI: 10.1039/c001950j

Six-dimensional dynamics study of reactive and non reactive scattering of H_2 from Cu(111) using a chemically accurate potential energy surface
C. Díaz, R. A. Olsen, D. J. Auerbach and G. J. Kroes, *Phys. Chem. Chem. Phys.*, 2010
DOI: 10.1039/c001956a

Azobenzene *versus* 3,3′,5,5′-tetra-*tert*-butyl-azobenzene (TBA) at Au(111): characterizing the role of spacer groups
Erik R. McNellis, Christopher Bronner, Jörg Meyer, Martin Weinelt, Petra Tegeder and Karsten Reuter, *Phys. Chem. Chem. Phys.*, 2010
DOI: 10.1039/c001978j

FTIR spectroscopy and thermodynamics of CO and H_2 adsorbed on γ-, δ- and α-Al_2O_3
Evgeniy N. Gribov, Olena Zavorotynska, Giovanni Agostini, Jenny G. Vitillo, Gabriele Ricchiardi, Giuseppe Spoto and Adriano Zecchina, *Phys. Chem. Chem. Phys.*, 2010
DOI: 10.1039/c002031c

A highly ordered, aromatic bidentate self-assembled monolayer on Au(111): a combined experimental and theoretical study
Xia Stammer, Katrin Tonigold, Asif Bashir, Daniel Käfer, Osama Shekhah, Christian Hülsbusch, Martin Kind, Axel Groß and Christof Wöll, *Phys. Chem. Chem. Phys.*, 2010
DOI: 10.1039/c002215m

Modelling active sites for the Beckmann rearrangement reaction in boron-containing zeolites and their interaction with probe molecules
Inés Lezcano-González, Alejandro Vidal-Moya, Mercedes Boronat, Teresa Blasco and Avelino Corma, *Phys. Chem. Chem. Phys.*, 2010
DOI: 10.1039/c002427a

A FTIR search for linkage isomerism of CN^- ions adsorbed on oxides and zeolites
A. A. Tsyganenko, A. M. Chizhik and A. I. Chizhik, *Phys. Chem. Chem. Phys.*, 2010
DOI: 10.1039/c003942j

Simultaneous adsorption of benzene and dioxygen in CuHY zeolites as a precursor process to the aerobic oxidation of benzene to phenol

Shampa Santra, Hermann Stoll and Guntram Rauhut*

Received 14th October 2009, Accepted 11th January 2010
First published as an Advance Article on the web 10th February 2010
DOI: 10.1039/b921531j

Possible precursor complexes for the aerobic oxidation of benzene to phenol in CuHY zeolites were studied by QM/MM calculations. Structures limited to just one copper center were determined, in which both, benzene and dioxygen are adsorbed to and activated by the same transition metal cation. Frequency analyses reveal that these complexes can be identified by the frequency shift of the O_2 stretching mode.

1. Introduction

The oxidation of benzene to phenol is an important industrial process, which is presently realized by the cumene process. Unfortunately this three-step reaction requires liquid inorganic acids and leads to a stoichiometric amount of acetone as a by-product. Consequently, more economical and ecological alternatives are sought that give rise to manifold activities in current research.[1–5] The search for cheap and commonly available oxidants on one side and a selective process on the other constitutes a bottleneck, which has not yet been removed. Phenol production by oxidation of benzene with molecular oxygen by using different catalysts in the gas- and liquid-phase has been described by several authors.[2–5] However, many of these reactions do not fulfil the second requirement—high selectivity. On the contrary, the oxidation of benzene by molecular oxygen on copper zeolites is characterized by very high selectivity. However, in comparison to other catalysts the yield averages to a few percent only for CuHY, CuHX and CuHZSM-5 zeolites.[2–5] Therefore, in order to increase the yield of phenol one needs to understand the reaction mechanism at the molecular level. This information would allow for a modification of the zeolite to favour phenol formation.

The mechanistic investigation of the aerobic oxidation of benzene to phenol in CuHY zeolites by computational methods is rather complicated and leads to a number of questions: (1) Where do the copper ions reside in the zeolite? (2) How many copper atoms are in direct neighborhood? (3) How relevant are dinuclear peroxo-complexes? (4) How many silicon atoms need to be replaced by aluminium atoms? (5) How does the aluminium distribution influence the reaction barrier? (6) Where do the protons needed for charge compensation reside? (7) Which is the most relevant adsorption site within the zeolite? (8) What is the most relevant electronic state for this reaction (triplet *vs.* singlet), when O_2 is used as an oxidant? (9) How does the zeolite have to be modified in order to accelerate the reaction? All these questions cannot be answered in a single study and thus a number of assumptions and side conditions must be introduced and the aspects to be studied need to be restricted. Previous studies of several groups showed that the most important adsorption sites in CuHY zeolites are the SII and SIII sites (for details see ref. 6 and 7). Apparently, the copper ion is bound more tightly at site SII than at site SIII. As a consequence the copper ion shows enhanced flexibility at site SIII which results in larger adsorption energies and thus a stronger activation of the reactive species. All this indicates that the SIII site is the preferred site for starting the reaction. Nevertheless, we initially focused on both, the SII and SIII sites. Again, previous studies showed that the triplet state appears to be lower in energy than the corresponding closed shell singlet states for adsorption complexes of O_2 and CuHY.[7] This assumption has been supported by multi-reference configuration interaction calculations as well as density functional studies.[7] However, both states are rather close in energy. For this very reason we focus mainly on the triplet state but consider the singlet states in certain cases as well.

The focus of the present study is not so much on the reaction itself but rather on adsorption complexes which may serve as a starting point for the reaction. The precursor complexes studied here are thought of as mimicking the experimental situation when a Cu-exchanged Y-zeolite is loaded by dioxygen and subsequently by benzene or *vice versa*. This addresses only a subset of the questions raised above but was found to be an important prerequisite for limiting the parameters controlling the reaction. In this preliminary study we restricted ourselves to the investigation of complexes with just one copper atom. The introduction of a second copper atom would result in a multitude of new structures and complicated electronic situations which are beyond the scope of this study and which are subject to further investigations. Whenever possible, we compare our calculations with our previous combined experimental/computational results on the *lone* adsorption of dioxygen *or* benzene to copper in CuHY zeolites.[7,8]

2. Computational details

A combined quantum mechanical (QM) and molecular mechanical (MM) approach (QM-Pot)[9,10] has been used. The QM region contains the adsorbates, the copper center

Institut für Theoretische Chemie, Universität Stuttgart, Pfaffenwaldring 55, 70569 Stuttgart, Germany

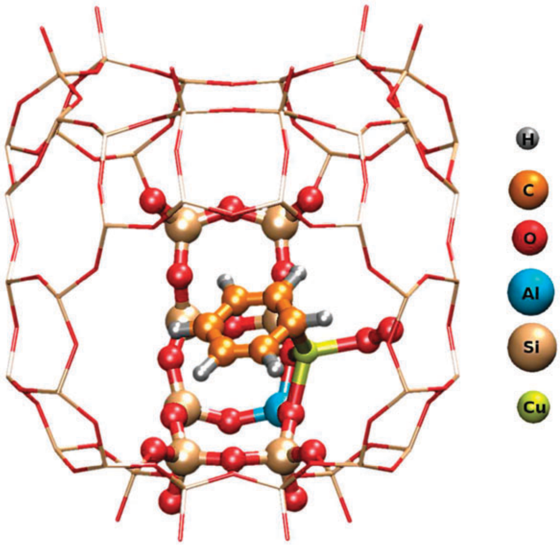

Fig. 1 QM/MM model of C_6H_6 and O_2 adsorbed in Cu-exchanged Y zeolite. Atoms computed at the DFT level are marked by balls.

and the zeolitic framework in the vicinity of the copper ion, while the MM part comprises the environment including the rest of all atoms of the periodic cell (see Fig. 1). In the QM/MM scheme of the QM-Pot program dangling bonds are saturated by hydrogen atoms connected to the terminating framework oxygen atoms, for the QM part. Periodic boundary conditions are applied to include long-range electrostatic effects, for the MM part.

Quantum chemical calculations were performed at the DFT (density functional theory) level employing the BP86 functional[14,15] and using the RI-*J* (resolution-of-identity) approximation[11–13] together with *valence triple ζ polarisation* (TZVP) orbital basis sets[16] for all O, Si, Al, H atoms. A relativistic small core ECP10MDF pseudopotential[17] with accompanying cc-pVTZ-PP basis sets[18] replaces the 10 innermost core electrons for the Cu atoms. An unrestricted Kohn–Sham (UKS) scheme was used for the triplet and broken-symmetry singlet states. For systems such as van der Waals (vdW) complexes found at site SII and SIII of Cu–Y zeolite (see Fig. 2 and 3) where dispersion interactions are decisive, we employed the DFT + D approach of Grimme and co-workers,[19] with parameters taken from ref. 20. DFT calculations were performed using the Turbomole[22,23] and Molpro[24] program packages, and MM calculations were performed with the Gulp program[25] linked to the QM-Pot program. The force field was parameterized using a polarizable ion-pair shell-model potential[26] with parameters developed by Sierka.[27] The interaction parameters for Cu(I) are: $A_{\mathrm{Cu(I)O}}$ = 2676.727189 eV and $\rho_{\mathrm{Cu(I)O}}$ = 0.24243 Å.[28] At the MM level van der Waals interactions between C_6H_6, dioxygen and the zeolite framework were modeled by Lennard-Jones 6–12 potentials with parameters taken from ref. 21.

The full unit cell of faujasite zeolite (Y zeolite) contains 192 Si/Al (called T atoms) atoms and 384 O atoms. However a smaller rhombohedral unit cell containing just 48 Si/Al atoms and 96 O atoms is taken in our present work. As in our previous study on the adsorption of O_2,[7] model clusters at two

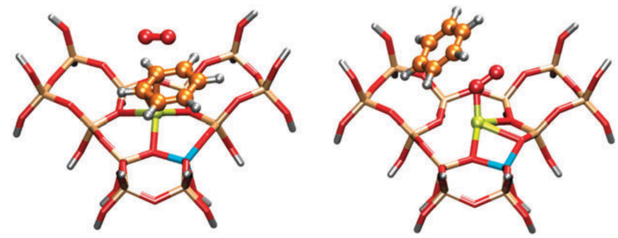

Fig. 2 Quantum mechanically treated part of van der Waals complexes formed at site SII: (lhs) direct connection of C_6H_6 to Cu, (rhs) direct connection of O_2 to Cu.

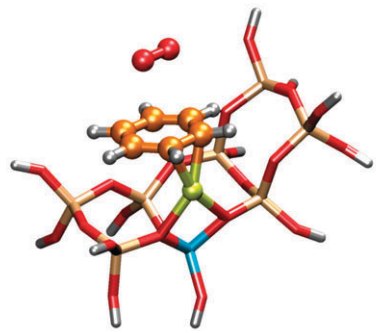

Fig. 3 Quantum mechanically treated part of van der Waals complexes formed at site SIII: direct connection of C_6H_6 to Cu.

different sites of Y zeolite were represented by 12 Si/Al atoms and 33 O atoms in case of site SII, and 8 Si/Al atoms and 22 O atoms in case of site SIII, respectively, treated at the DFT level. The QM part of the Y zeolite model contains one or two Al atoms, whereas the embedding part of it is pure silica. In case of 2 Al clusters, an additional H^+ ion is incorporated in order to neutralize the charge of the zeolite. Distribution of the second Al atom follows the Loewenstein rule,[29] *i.e.*, Al–O–Al connectivity is excluded. After introduction of the 2nd Al into the model clusters (which are embedded within the zeolite framework), site SIII gives 9 isomers depending on the position of the two Al atoms to each other. The isomers are individually characterized by specifying the Si atom which are replaced by the 2nd Al atom and the O atoms to which the additional proton is connected in Table 1 and 2. The numbering of the atoms used here and in the following refers to crystallographic labeling (considering the four different zeolitic–O positions O1, O2, O3, O4) with an additional letter used for identifying individual atoms (see Fig. 4). For detailed information concerning basis set effects see ref. 7, and for our investigations concerning other adsorbates (ethene and ethyne) based on finite cluster models see ref. 30 and 31.

3. Results and discussion

3.1 Structural and energetical aspects

Geometry optimizations were performed for sites SII and SIII with benzene and dioxygen located at positions within the supercage, which are in the vicinity of the Cu(I) ion. For both sites we found van der Waals complexes in the triplet state in which the dioxygen molecule resides on top of the benzene ring, which itself is bound to the copper ion. For an illustration

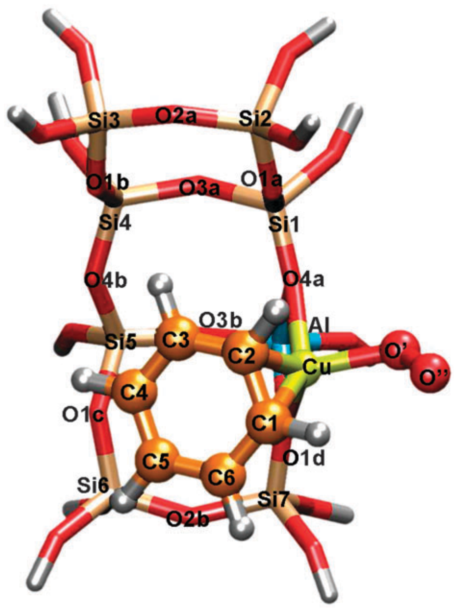

Fig. 4 Numbering of the atoms of the Cu–exchanged Y zeolite skeleton in the QM region containing only 1 Al atom. The second Al atom replaces any of the Si atoms except the neighbouring ones.

see Fig. 2 and 3. For site SII another local minimum has been found in which the O_2 molecule is directly bound to the copper ion while benzene floats on top of this moiety (see Fig. 2, right). Obviously it matters if in the experiment the zeolite is first loaded with benzene and subsequently by dioxygen or the other way around. Although these complexes keep the dioxygen in close proximity to benzene, they have of course little relevance for the reaction of benzene to phenol and will only be considered briefly in the following.

Other complexes than these were only found for site SIII where both O_2 and C_6H_6 are connected to the same copper center and thus we focus exclusively on this site in the remainder of this paper. Three sets of geometry optimizations were performed for the different electronic states, *i.e.*, the triplet, closed shell singlet and broken-symmetry singlet states. For each electronic state the number and position of aluminium atoms and of the corresponding charge-conserving protons were varied. This resulted in a total of 27 structures for each complex. We found two structurally very similar complexes whose structures are characterized in Table 1 and 2 and which are displayed in Fig. 5. These systems are closely related to complexes of Datka and co-workers,[32,33] who studied the simultaneous adsorption of CO or NO and some organic

Table 1 Relative energies^a (E_{rel}), binding energies ($E_b{}^b$ and $E_b{}^c$) of C_6H_6 + O_2 at site SIII for different electronic states (in kcal mol^{-1}). All data refer to the complex lower in energy (see Fig. 5, lhs). The results in the first line refer to the case of 1 Al atom in a ring and the others to different isomers with 2 Al atoms

			Triplet			BS singlet			Singlet		
Isomers	2nd Al atom replaces	H atom is connected to	E_{rel}	$E_b{}^b$	$E_b{}^c$	E_{rel}	$E_b{}^b$	$E_b{}^c$	E_{rel}	$E_b{}^b$	$E_b{}^c$
1 Al	—	—		−37.0	−3.4		−31.0	2.5		−15.8	17.7
A	Si2	O1a	5.9	−44.6	−5.9	6.1	−38.6	0.2	5.3	−24.9	13.9
B	Si2	O2a	2.2	−35.6	−2.8	2.5	−29.6	3.2	3.4	−14.0	18.7
C	Si3	O2a	0.0	−38.5	−4.4	0.0	−32.7	1.4	0.0	−18.2	16.0
D	Si3	O1b	6.8	−36.6	−1.6	7.3	−30.3	4.7	9.2	−13.9	21.1
E	Si4	O1b	9.6	−34.4	−0.03	9.7	−28.6	5.8	10.1	−13.6	20.8
F	Si4	O3a	28.3	−38.3	−4.2	28.3	−32.5	1.6	28.9	−17.3	16.8
G	Si4	O4b	10.9	−36.1	−0.4	11.2	−29.9	5.8	12.4	−14.2	21.4
H	Si6	O1c	0.6	−36.7	−3.6	0.7	−30.7	2.3	1.1	−15.7	17.3
I	Si6	O2b	2.0	−38.6	−3.5	2.3	−32.5	2.6	3.6	−16.7	18.4

^{a} E_{rel} of different isomers are defined with respect to the lowest energy isomer. ^{b} Binding energy with respect to isolated benzene, dioxygen and CuHY. ^{c} Binding energy of dioxygen with respect to benzene adsorbed to CuHY.

Table 2 Relative energies^a (E_{rel}), binding energies ($E_b{}^b$ and $E_b{}^c$) of C_6H_6 + O_2 at site SIII for different electronic states (in kcal mol^{-1}). All data refer to the 2nd complex (see Fig. 5, lhs). The results in the first line refer to the case of 1 Al atom in a ring and the others to different isomers with 2 Al atoms

			Triplet			BS Singlet			Singlet		
Isomers	2nd Al atom replaces	H atom is connected to	E_{rel}	$E_b{}^b$	$E_b{}^c$	E_{rel}	$E_b{}^b$	$E_b{}^c$	E_{rel}	$E_b{}^b$	$E_b{}^c$
1 Al	—	—		−36.3	−2.8		−30.2	3.4		−20.4	13.2
A	Si2	O1a	6.3	−43.4	−4.7	8.1	−37.2	1.6	5.8	−27.5	11.3
B	Si2	O2a	0.8	−36.2	−3.4	2.6	−30.0	2.7	1.1	−19.5	13.3
C	Si3	O2a	1.7	−36.1	−1.9	3.4	−29.9	4.2	1.3	−20.0	14.1
D	Si3	O1b	6.7	−35.9	−1.0	8.5	−29.7	5.2	4.5	−21.6	13.3
E	Si4	O1b	8.7	−34.6	−0.20	10.4	−28.4	6.0	6.8	−20.1	14.3
F	Si4	O3a	16.8	−48.9	−14.8	18.6	−42.8	8.7	28.3	−21.1	13.0
G	Si4	O4b	9.9	−36.3	−0.6	11.7	−30.1	5.6	12.2	−17.5	18.1
H	Si6	O1c	0.0	−36.4	−3.3	0.0	−32.0	1.0	0.0	−20.0	13.1
I	Si6	O2b	2.3	−37.6	−2.5	4.0	−31.4	3.7	4.5	−18.9	16.2

^{a} E_{rel} of different isomers are defined with respect to the lowest energy isomer. ^{b} Binding energy with respect to isolated benzene, dioxygen and CuHY. ^{c} Binding energy of dioxygen with respect to benzene adsorbed to CuHY.

molecules in CuZSM-5 zeolites. These two complexes shown in Fig. 5 differ by just 0.6 kcal mol^{-1} (triplet state, one Al atom in the inner ring) in favor of the first structure (Fig. 5, lhs). All structures provided in Table 1 and 2 are characterized by an η^2-coordination of benzene and end-on orientation of dioxygen. As an example, Table 3 shows detailed information of the geometrical parameters for the triplet clusters containing just one aluminium atom. For comparison the corresponding structural parameters of clusters with solely adsorbed dioxygen *or* benzene are given as well. This comparison shows that the clusters containing benzene *and* dioxygen are closely related to those containing just one adsorbate. Obviously only slight distortions (which require a minor reorganization energy) are needed to allow for the lone adsorption of both molecules. The most prominent change with respect to a cluster containing dioxygen as lone adsorbate is the change of a side-on coordination in favor of an end-on coordination (yielding a reduction of the O_2 bond length comparable to that for the end-on adsorption of lone dioxygen at the SII adsorption site[7]). This in turn leads to a five-fold coordination of the Cu(I) ion. The introduction of a second Al atom leads to model systems closer to the real situation in Cu-containing faujasites where a Si/Al ratio of 2.2 to 2.4 is observed. Consequently, for the first complex (Fig. 5, lhs) the most relevant structure of this study appears to be cluster C, in which the 2nd Al atom replaces Si3 while the additional proton is connected to O2a (*cf.* Table 1). Cluster H is still very close in energy (within 1 kcal mol^{-1}), while all other systems are off by at least 2.0 kcal mol^{-1}. These results appear to be independent of the electronic state: structure C is also the minimum lowest in energy for the closed shell and broken-symmetry singlet states. For the second complex the situation is very similar: Again the proton is located at an O2 or O1 position, but the preferred position for the 2nd Al atom is now Si6 instead of Si3. In all cases, the binding energy—computed as the difference of the cluster with respect to the three isolated systems with dioxygen being in the triplet state—of the clusters in the triplet state is significantly larger than for the corresponding closed shell singlet state. The binding energies of the broken-symmetry singlet states are always fairly close to the triplet states. We attribute this result to a significant admixture of triplet contributions to the singlet states. However, these results confirm our principal restriction to triplet states and thus our further considerations focus exclusively on triplet state calculations. This is in line with our recent high-level benchmark calculations at the coupled-cluster and multi-reference configuration interaction level.[7] Recently, Holthausen and co-workers[34] investigated the interaction of the copper ion with substituted benzenes and compared the DFT with CCSD(T) results showing a fairly good agreement. Moreover, binding energies of dioxygen with respect to benzene adsorbed to CuHY are positive for all complexes in the singlet and the symmetry broken singlet state. Consequently, in these electronic states the formation of the clusters is very unlikely once the zeolite has been loaded with benzene prior to the addition of dioxygen. For the low-lying triplet states of the two complexes, we observe an energy stabilization of 3–4 kcal mol^{-1} with respect to benzene adsorbed to CuHY and free dioxygen.

We consider the clusters shown in Fig. 5 potential precursor complexes for the oxidation of benzene to phenol for several

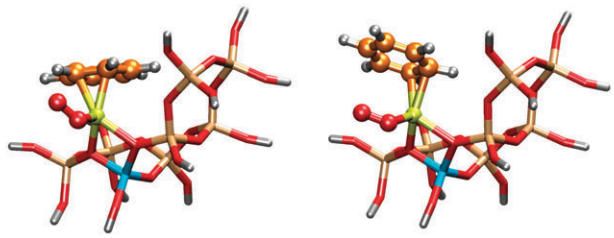

Fig. 5 Quantum mechanically treated part of possible precursor complexes (containing 1 Al atom) for the aerobic oxidation of benzene to phenol formed at site SIII.

reasons: (1) Both adsorbates are activated which is certainly more favorable than activating just one entity. (2) Oxygen atom O″ is in very close neighbourhood to the activated CC bond of benzene which allows for a direct reaction. (3) All structures were found to be very flexible and floppy, allowing for structural reorientations without significant changes in energy.

3.2 Population analysis

A central question refers to the oxidation state of the copper ion. Note that we did not impose any constraint to that aspect except charge neutrality of the entire system in our calculations. We performed population analyses for all three electronic states for isomers C and H using the natural orbital scheme of Reed and Weinhold[35] as implemented in TURBOMOLE. In all cases the copper ion carries a positive charge between 1.12 and 1.11 and thus must be considered a Cu(I) ion. The O″ atoms are negatively charged by about −0.08. Therefore the O″ atom interacts directly with the positively charged hydrogen atoms of benzene. In both clusters the 3d4s occupation of the copper ion is $3d^{9.61}4s^{0.26}$. In order to study the oxidation state of copper in more detail, we augmented our calculations by the following scheme: in the calculations for the first complex with a 2nd Al atom at position Si6 (formally referring to structures H or I), we removed the proton from the Brønsted site *and* an (additional) electron. This situation refers to a doublet state and is supposed to remove the electron from the copper ion in order to form Cu(II). After a geometry optimization of this cluster we performed natural population analysis. The charge of the copper ion was found to be 1.15 and thus the electron has been removed from the zeolite skeleton rather than the copper. The occupation pattern of the copper ion did also hardly change, *i.e.*, $3d^{9.58}4s^{0.26}$. According to these tests the preferred oxidation state for copper in these complexes appears to be Cu(I) rather than Cu(II), but the spin density at the copper atom is non-zero (0.2–0.3).

3.3 Vibrational frequencies

In the van der Waals complexes discussed above the dioxygen molecule is only loosely bound to the benzene moiety and thus one would not expect significant frequency shifts for these structures. According to our calculations the O_2 stretching mode is red shifted by 39 cm^{-1} from 1556 to 1517 cm^{-1} (after scaling, *cf.* Tables 4 and 5 for the scaling factors used). This shift is significantly larger than that computed for the end-on adsorption of dioxygen to a Brønsted center, which is in the

Table 3 Geometrical parameters (given in Å) for the adsorption of benzene and dioxygen at SIII position for the case of 1 Al atom in the neighboring skeleton of T-atoms. For the numbering of the atoms refer to Fig. 4

	Adsorption of O_2 and C_6H_6				
Parameters	1st Minimum[b]	2nd Minimum[c]	Adsorption of O_2 only	Adsorption of C_6H_6 only	Bare cluster
O′–O″	1.262	1.259	1.318		
O″–C1	3.303	3.364			
O″–C2	3.627	3.321			
O″–H[a]	2.618	3.688			
Cu–O′	1.978	1.962	1.971		
Cu–O″	2.882	2.855	1.940		
Cu–O4a	2.207	2.226	2.019	2.165	2.035
Cu–O1d	2.053	2.052	1.968	2.016	1.982
Cu–Al	2.909	2.911	2.799	2.862	2.737
Cu–C1	2.208	3.586		2.071	
Cu–C2	2.137	3.617		2.024	
Cu–C3	2.821	3.013		2.695	
Cu–C4	3.412	2.189		3.261	
Cu–C5	3.472	2.154		3.320	
Cu–C6	2.951	2.950		2.810	

[a] Nearest H atom of benzene ring. [b] Fig. 5, lhs. [c] Fig. 5, rhs.

range of 0–8 cm^{-1}.[7] Note that the O_2 stretching mode is extremely sensitive with respect to environmental effects: considering the adsorption of dioxygen to the copper ion at the SIII site, the frequency shift of the O_2 stretching mode (with respect to free dioxygen in the gas-phase and without a simultaneous benzene adsorption) is about 380 cm^{-1}.[7]

With respect to the precursor complexes shown in Fig. 5 our frequency calculations result in O_2 stretching modes between 1330 and 1359 cm^{-1} (after scaling)—in dependence on the aluminium distribution patterns (*cf.* Tables 4 and 5). This corresponds to frequency shifts between 226 and 197 cm^{-1} in contrast to 380 cm^{-1} as observed for the lone adsorption of dioxygen. However, the frequency shift of 380 cm^{-1} was found for a side-on adsorption at the SIII site. End-on adsorption of dioxygen to copper at site SII results in frequency shifts (in dependence on the Al distribution) between 258 and 321 cm^{-1}. Consequently, the reduced frequency shift from 380 cm^{-1} to values between 226 and 197 cm^{-1} for site SIII does not only result from a reorientation (side-on to end-on) of the O_2 molecule, but also from the benzene adsorption. This reveals that the interaction of dioxygen with the copper ion is markedly weaker than in the case of pure O_2 adsorption. Consequently, the benzene molecule has to interact directly with the copper ion as well as with the dioxygen molecule which leads to the observed lowering of the frequency shift. In complexes with two copper ions (which are not studied here), in which the dioxygen molecule is adsorbed to one copper ion and the benzene to the other, the O_2 frequency shift should be stronger than that computed here and thus IR spectroscopy should be able to distinguish between these different situations. However, this of course holds true only in case that the lifetime of the computed complexes is long enough and that the IR signals are markedly different from other intermediates or reaction products of the benzene oxidation. In general, one has to expect spectra arising from a multitude of different complexes. *In situ* IR experiments are currently performed to

Table 4 Simultaneous adsorption of C_6H_6 and O_2 at site SIII of CuHY zeolite. Comparison of calculated harmonic frequencies ν and frequency shifts $\Delta\nu$ (in cm^{-1}) of benzene and O_2 in gas-phase and adsorbed state. Geometries and analytic force constants are calculated at BP86/TZVP level; within the RI-*J* approximation. Scaling factors are 1.012 and 1.02 for C_6H_6 and O_2, respectively. All data refer to the complex lower in energy (see Fig. 5, lhs)

	C_6H_6		O_2	
	ν_{13} (C–C ring stretch)	$-\Delta\nu_{13}$[a]	ν_{O-O} (O–O stretch)	$-\Delta\nu_{O-O}$[b]
Gas-phase	1489		1556	
Cu(SIII)HY/1Al	1473/1471	16/18	1335	221
Cu(SIII)HY/2Al				
A	1473/1469	16/20	1345	211
B	1473/1470	16/19	1341	215
C	1476/1473	13/16	1329	227
D	1473/1467	16/22	1359	197
E	1474/1471	15/18	1330	226
F	1474/1472	15/17	1334	222
G	1472/1468	17/21	1350	206
H	1472/1469	17/20	1337	219
I	1472/1471	17/18	1343	213

[a] $\Delta\nu$ is the frequency shift of benzene from the gas-phase to the adsorbed state. [b] $\Delta\nu_{o-o}$ is the frequency shift of O_2 from the gas-phase to the adsorbed state.

Table 5 Simultaneous adsorption of C_6H_6 and O_2 at site SIII of CuHY zeolite for second type of co-adsorption complexes. Comparison of calculated harmonic frequencies ν and frequency shifts $\Delta\nu$ (in cm^{-1}) of benzene and O_2 in gas-phase and adsorbed state. Geometries and analytic force constants are calculated at BP86/TZVP level; within the RI-*J* approximation. Scaling factors are 1.012 and 1.02 for C_6H_6 and O_2, respectively. All data refer to the 2nd complex (see Fig. 5, right)

	C_6H_6		O_2	
	ν_{13} (C–C ring stretch)	$-\Delta\nu_{13}$ [a]	ν_{O-O} (O–O stretch)	$-\Delta\nu_{O-O}$ [b]
Gas-phase	1489		1556	
Cu(SIII)HY/1Al	1475/1471	14/18	1346	210
Cu(SIII)HY/2Al				
A	1477/1472	12/17	1346	210
B	1477/1473	12/16	1345	211
C	1477/1473	12/16	1341	215
D	1475/1474	14/15	1348	208
E	1474/1473	15/16	1342	214
F	1476/1473	13/16	1348	208
G	1475/1472	14/17	1348	208
H	1475/1475	14/14	1330	226
I	1481/1474	8/15	1345	211

[a] $\Delta\nu$ is the frequency shift of benzene from the gas-phase to the adsorbed state. [b] $\Delta\nu_{o-o}$ is the frequency shift of O_2 from the gas-phase to the adsorbed state.

identify a new band in the region discussed above or band shifts once benzene is added.[36]

Besides the discussion of the O_2 stretching modes, we will consider the ν_{13} band of benzene (*cf*. Tables 4 and 5). This degenerate mode is significantly less sensitive than the O_2 stretching mode and leads to pairs of transitions due to the symmetry breaking of the benzene molecule upon adsorption. Similar to the O_2 stretching mode, the frequency shift of the ν_{13} mode in comparison to the shift in the lone adsorption of benzene is markedly smaller.[8] The same holds true for splitting of the mode, which reduces from about 8 to 3 cm^{-1}. Again this indicates a weaker interaction of the benzene molecule with the copper ion in comparison to the lone adsorption of benzene at site SIII. As a result one would expect a subtle blue shift in the experimental IR spectra once oxygen is added to a benzene loaded CuHY zeolite.

The frequency analysis performed above indicates that *in situ* IR experiments are capable of providing valuable information about possible precursor complexes relevant for the oxidation of benzene to phenol in Y-zeolites. In particular the O–O stretching mode—to be expected in the region around 1340 cm^{-1}—acts as a sensitive indicator. Once an experimental band has been found in this region one may conclude that (a) site SIII is the most relevant adsorption site and (b) that the complexes discussed here may indeed be involved in the catalytic cycle forming phenol.

4. Summary and conclusions

Possible precursor complexes for the CuHY catalyzed aerobic oxidation of benzene to phenol were determined by QM/MM calculations at the DFT level. These complexes involve just one copper center and lead to a simultaneous adsorption to the same copper atom and activation of both molecules, dioxygen *and* benzene at site III of the Cu–Y zeolite. Most likely, these complexes are relevant precursor complexes for the oxidation of benzene to phenol. Pulido *et al.* have been recently investigating the direct NO decomposition on Cu/zeolites, and reported that Cu(I) *coordinated inside a flexible* (*non-bridged*) *six-membered ring* (*such as the P6/T1 site*) *shows lower or no activity*.[37] This agrees quite nicely with our results, *i.e.*, precursor complexes have been characterized solely at site III (bridged-4-ring) rather than at site II (6-ring). The complexes are characterized by a distinct O_2 stretching mode, which is red shifted with respect to dioxygen in the gas phase but blue shifted with respect to the lone adsorption of dioxygen in CuHY zeolites. Moreover, van der Waals complexes were found, in which the benzene and the dioxygen molecules reside on top of each other. These complexes result in a rather modest red shift of the dioxygen stretching mode. As the reaction mechanism of the aerobic oxidation of benzene to phenol in CuHY zeolites is still unknown, these determined complexes constitute an interesting starting point for alternative reaction channels in contrast to reactions involving two copper ions. However, in order to pinpoint the importance of the clusters of this study for the aerobic oxidation of benzene to phenol the whole reaction path needs to be investigated. Work in that direction is currently in progress.

Acknowledgements

The authors thank Prof. E. Roduner and T. Archipov for many helpful discussions. This work was performed within the Collaborative Research Centre SFB 706 (Selective Catalytic Oxidations Using Molecular Oxygen; Stuttgart) and funded by the German Research Foundation. Computer time at the Institut für Theoretische Chemie der Universität Stuttgart is kindly acknowledged.

References

1 M. Ivamoto, J. Hirata, K. Matsukami and S. Kagawa, *J. Phys. Chem.*, 1983, **87**, 903.
2 R. Hamada, Y. Shibata, S. Nishiyama and S. Tsuruya, *Phys. Chem. Chem. Phys.*, 2003, **5**, 956.
3 T. Kitamura, H. Kanzaki, S. Nishiyama and S. Tsuruya, *Can. J. Chem.*, 2004, **82**, 1597.

4 N. B. Castagnola, A. J. Kropf and C. L. Marshall, *Appl. Catal., A*, 2005, **290**, 110.
5 Y. Shibata, R. Hamada, T. Ueda, Y. Ichihashi, S. Nishiyama and S. Tsuruya, *Ind. Eng. Chem. Res.*, 2005, **44**, 8765.
6 P. Rejmak, M. Sierka and J. Sauer, *Phys. Chem. Chem. Phys.*, 2007, **9**, 5446.
7 S. Santra, T. Archipov, A. B. Ene, H. Komnik, H. Stoll, E. Roduner and G. Rauhut, *Phys. Chem. Chem. Phys.*, 2009, **11**, 8855.
8 T. Archipov, S. Santra, A. B. Ene, H. Stoll, G. Rauhut and E. Roduner, *J. Phys. Chem. C*, 2009, **113**, 4107.
9 J. Sauer and M. Sierka, *J. Comput. Chem.*, 2000, **21**, 1470.
10 M. Sierka and J. Sauer, *J. Chem. Phys.*, 2000, **112**, 6983.
11 K. Eichkorn, O. Treutler, H. Öhm, M. Häser and R. Ahlrichs, *Chem. Phys. Lett.*, 1995, **240**, 283.
12 K. Eichkorn, O. Treutler, H. Öhm, M. Häser and R. Ahlrichs, *Chem. Phys. Lett.*, 1995, **242**, 652.
13 K. Eichkorn, F. Weigend, O. Treutler and R. Ahlrichs, *Theor. Chem. Acc.*, 1997, **97**, 119.
14 A. D. Becke, *Phys. Rev. A: At., Mol., Opt. Phys.*, 1988, **38**, 3098.
15 J. P. Perdew, *Phys. Rev. B: Condens. Matter*, 1986, **33**, 8822.
16 A. Schäfer, C. Huber and R. Ahlrichs, *J. Chem. Phys.*, 1994, **100**, 5829.
17 D. Figgen, G. Rauhut, M. Dolg and H. Stoll, *Chem. Phys.*, 2005, **311**, 227.
18 K. A. Peterson and C. Puzzarini, *Theor. Chem. Acc.*, 2005, **114**, 283.
19 S. Grimme, *J. Comput. Chem.*, 2004, **25**, 1463.
20 S. Grimme, *J. Comput. Chem.*, 2006, **27**, 1787.
21 J. O. Hirschfelder, C. F. Curtiss and R. B. Bird, *Molecular Theory of Gases and Liquids*, John Wiley & Sons, New York, Chapman & Hall, London, 1954, p. 1112.
22 R. Ahlrichs, M. Bär, M. Häser, H. Horn and C. M. Kölmel, *Chem. Phys. Lett.*, 1989, **162**, 165.
23 O. Treutler and R. Ahlrichs, *J. Chem. Phys.*, 1995, **102**, 346.
24 MOLPRO, Development Version 2006.2, is a package of *ab initio* programs written by H.-J. Werner and P. J. Knowles, with contributions from R. D. Amos, A. Bernhardsson, A. Berning, P. Celani, D. L. Cooper, M. J. O. Deegan, A. J. Dobbyn, F. Eckert, C. Hampel, G. Hetzer, T. Korona, R. Lindh, A. W. Lloyd, F. R. Manby, W. Meyer, S. J. McNicholas, M. E. Mura, A. Nicklass, P. Palmieri, K. Peterson, P. Pulay, G. Rauhut, M. Schütz, U. Schumann, H. Stoll, A. J. Stone, R. Tarroni and T. Thorsteinsson, (see http://www.molpro.net/).
25 J. D. Gale, *J. Chem. Soc., Faraday Trans.*, 1997, **93**, 629.
26 R. A. Jackson and C. R. A. Catlow, *Mol. Simul.*, 1988, **1**, 207.
27 M. Sierka and J. Sauer, *Faraday Discuss.*, 1997, **106**, 41.
28 D. Nachtigallová, P. Nachtigall, M. Sierka and J. Sauer, *Phys. Chem. Chem. Phys.*, 1999, **1**, 2019.
29 W. Loewenstein, *Am. Mineral*, 1954, **39**, 92.
30 G. Hübner, G. Rauhut, H. Stoll and E. Roduner, *Phys. Chem. Chem. Phys.*, 2002, **4**, 3112.
31 G. Hübner, G. Rauhut, H. Stoll and E. Roduner, *J. Chem. Phys. B*, 2003, **107**, 8586.
32 J. Datka, E. Kukulska-Zajac and W. Kobyzewa, *Catal. Today*, 2006, **114**, 169.
33 P. Kozyra and J. Datka, *THEOCHEM*, 2006, **778**, 35.
34 P. Milko, J. Roithová, D. Schröder, J. Lemaire, H. Schwarz and M. C. Holthausen, *Chem.–Eur. J.*, 2008, **14**, 4318.
35 NBO program: E. D. Glendening, A. E. Reed, J. E. Carpenter, F. Weinhold, A. E. Reed, L. A. Curtiss and F. Weinhold, *Chem. Rev.*, 1988, **88**, 899.
36 T. Archipov, A. B. Ene and E. Roduner, to be published.
37 A. Pulido and P. Nachtigall, *Chem. Cat. Chem.*, 2009, **1**, 449.